

Communications

Ultrawideband (UWB) Antennas With Multiresonant Split-Ring Loops

G. M. Yang, R. H. Jin, G. B. Xiao, C. Vittoria, V. G. Harris, and N. X. Sun

Abstract—Novel ultrawideband (UWB) antennas with multiresonant split-ring loops and with coplanar waveguide (CPW) feed are presented in this communication. Dual concentric microstrip split-ring loops with different geometrical ground planes have been analyzed and compared. UWB antennas are designed, of which the dimension of each split-ring loop varies proportionally to the arithmetic progression sequence. The dimensions of the rectangular ground planes and the split-ring loops are tuned for achieving a very wide bandwidth. A tapered transmission line is adopted to improve the return loss performance in the required band. Measurement results show that the proposed UWB antennas have a wide bandwidth from 2 to 20 GHz, and the measured return losses are less than -10 dB in this band combined with relative stable radiation characteristics.

Index Terms—Coplanar waveguide (CPW), split-ring loops (SRLs), ultrawideband (UWB) antenna.

I. INTRODUCTION

In recent years, with the continuous growth of ultrawideband (UWB) wireless communication technologies, design and manufacturing of low cost microwave components are among most critical issues in communication systems [1], [2]. UWB technology can be widely used in ground penetrating radars, high data rate short wireless local area communications, parking radars, and other military applications. As a very important passive component in ultrawideband wireless communications, UWB antennas with good radiation patterns and impedance matching are becoming highly desired both in industry and academia [3]–[7]. In [3], a bi-arm rolled monopole antenna, which was realized by wrapping a planar monopole, has been adopted for the UWB applications. The designed monopole antenna can achieve a broadband, omnidirectional radiation characteristics and with a simple structure. However, they are not planar structures as they were set above a big ground plane, and not easily integrated with RF integrated circuit. In [4], a simple microstrip antenna was investigated for the UWB wireless communication system, which has decent radiation pattern. However, its frequency performance is not so good at high frequency, since the microstrip antenna is not so good a candidate for wideband antenna. Coplanar waveguide (CPW) fed UWB antennas are supposed to be better candidates because of their simple configuration, manufacturing advantages, repeatability and low cost [5]–[7]. Another advantage is that the characteristic impedance of the feed line is determined by the ratio of the line width and the width of the gap between the ground plane and feed line. In [5], CPW-fed circular disc

Manuscript received May 08, 2007; revised October 05, 2008. Current version published March 04, 2009.

G. M. Yang, C. Vittoria, V. G. Harris, and N. X. Sun are with the Department of Electrical and Computer Engineering, Northeastern University, Boston, MA 02115 USA (e-mail: guomyang@hotmail.com).

R. H. Jin and G. B. Xiao are with the Department of Electronic Engineering, Shanghai Jiao Tong University, Shanghai 200240, China.

Digital Object Identifier 10.1109/TAP.2008.2009744

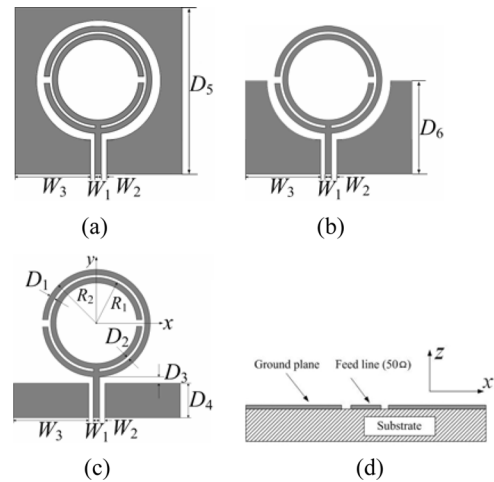


Fig. 1. Geometry of the printed monopole antenna. (a) Circular ground plane. (b) Semicircular ground plane. (c) Rectangular ground plane. (d) Side view of the CPW-fed antenna. $W_1 = 3.15$, $W_2 = 0.55$, $W_3 = 26$, $D_1 = 2.1$, $D_2 = 0.6$, $D_3 = 0.2$, $D_4 = 13$, $D_5 = 54$, $D_6 = 30$, all in mm.

monopole antenna has been realized for the UWB application, the effect of the disc and the ground planes has been investigated. However, since there is only one resonant structure in the design, it is not so easy to align the multiple resonance modes in the working frequency. In [6] and [7], fractal technique and triangle ground plane have been utilized to obtain a very wide frequency band, and UWB antennas have been successfully designed fulfilling the FCC's requirements.

To satisfy the UWB requirements, an effective method to design the wide-band antenna is to use multiresonant elements [8]. Annular-ring slot structure is adopted to design dual frequency antennas in [9] and [10]. A dual concentric microstrip annular ring can be considered as a complementary structure of the dual concentric annular ring slots. If the symmetry of the annular ring is disturbed, the degenerate resonant modes will be excited. In this communication, a new structure with multiresonant split-ring loops is proposed, and antennas with different geometrical ground planes have been compared in order to achieve a very wide bandwidth. Then the radiation patterns with different geometrical dimensions of the rectangular ground planes and different values of the radii of the split-ring loops are analyzed. Based on these analyses, an UWB antenna was fabricated and measured. The measured results show that the designed UWB antenna has a full frequency band from 2.0 to 20 GHz, and the fractional bandwidth is about 160% with a central frequency of 11 GHz. It also yields good radiation patterns in the whole frequency band and with a compact size of 36 mm by 49 mm.

II. ANTENNA DESIGN AND PERFORMANCE

Fig. 1(a)–(c) shows three kinds of antennas with dual concentric split-ring loops and CPW feed. Based on the dual concentric slots antenna in [10], we proposed a complementary structure of dual concentric microstrip split-ring loops, as shown in Fig. 1(a). Split-ring loops antennas with semicircular ground and rectangular ground planes are proposed, as shown in Fig. 1(b) and (c), respectively. Each antenna consists of a pair of concentric split-ring loops, a $50\text{-}\Omega$ CPW fed line and the ground planes. Both split-ring loops and the CPW feed line are realized by patterned copper cladding formed on the top surface of the

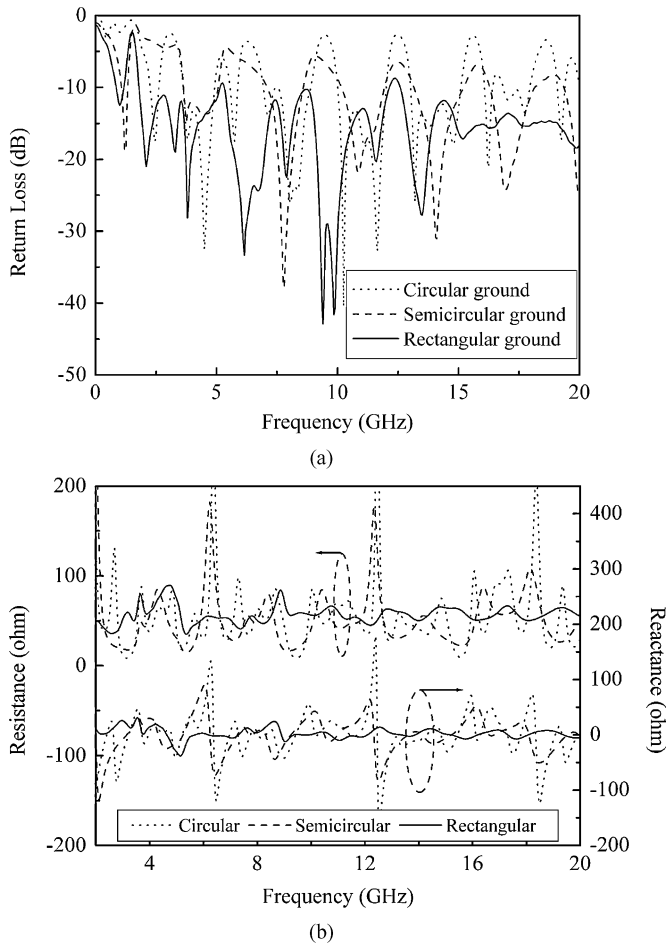


Fig. 2. (a) Simulated return loss curves for different geometrical ground planes. (b) Simulated impedance curves.

underlying dielectric substrate. All these antennas have the same dimensions, except that they have different geometrical ground planes. In this figure, R_1 and R_2 are the radii of the inner and outer split ring, respectively. D_1 is the width of the ring, D_2 is the gap between these two split rings, and D_3 is the distance between the outer ring and the ground plane. In this paper, the relative dielectric substrate is 2.65 with a thickness of 1 mm. W_1 and W_2 are fixed at 3.15 and 0.55 mm, respectively, in order to obtain a 50- Ω input impedance.

As shown in Fig. 2(a), antenna with circular plane has multiple resonance modes. Since the current is distributed mainly along the edge of the loops and the ground plane, we can obtain a very wide frequency band and improve the impedance matching by adjusting the geometry of the ground plane to decrease the capacitive effect. Therefore semi-circular ground and rectangular ground planes are proposed, as shown in Fig. 1(b) and (c), and investigated in this paper. We can see from Fig. 2(b) that the antenna with rectangular ground plane has better impedance matching than the others.

The radiation pattern, which is another important characteristic in the antenna design, depends heavily on the dimensions of the ground plane for our split-ring loop antenna. Fig. 3(a)–(d) shows the far-field radiation patterns in the azimuth plane with different dimensions of W_3 of rectangular ground plane. It is shown that the main radiation patterns remain similar, while with the increases of the length of the ground plane, the minor side lobe in the back of the ground plane decreases at low frequency. Also when the frequency increases beyond 7 GHz, the radiation patterns start to change and show higher directivities in other directions. Fig. 3(b)–(d) shows the simulated radiation patterns

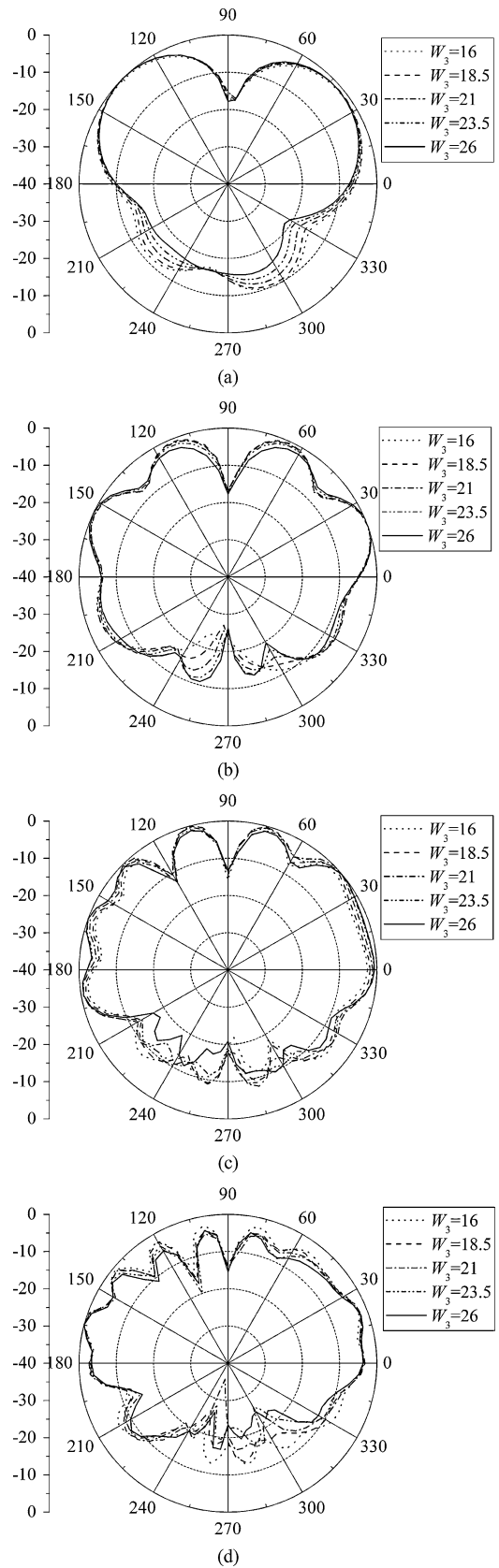


Fig. 3. Radiation patterns of azimuth plane (x-y plane) of the proposed antenna with rectangular ground plane. (a) 3 GHz. (b) 7 GHz. (c) 11 GHz. (d) 15 GHz.

of the antenna in the azimuth plane. As frequency increases, the electrical dimensions of the antenna increase and as a result, the number of

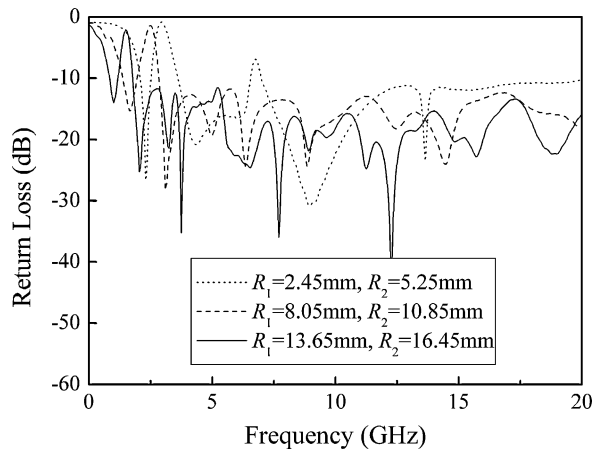


Fig. 4. Simulated return loss curves for different values of radii.

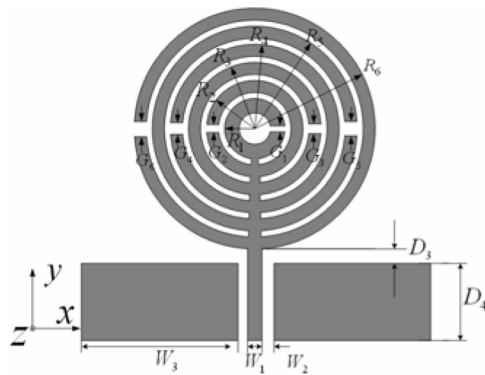


Fig. 5. CPW-fed printed UWB antenna. $R_1 = 2.45$, $R_2 = 5.25$, $R_3 = 8.05$, $R_4 = 10.85$, $R_5 = 13.65$, $R_6 = 16.45$, $G_1 = 0.6$, $G_2 = 1.0$, $G_3 = 1.4$, $G_4 = 1.8$, $G_5 = 2.2$, $G_6 = 2.6$, all in mm.

lobes increases. Also, the number of the minor side lobes in the back of the ground plane increases significantly. This is caused by diffractions from the edges of the ground plane, which has large electrical dimensions at higher frequencies. At lower frequencies, the radiation patterns are symmetric; however, as frequency increases, the symmetry is not observed very well. In order to keep the radiation pattern at the main radiation pattern direction and minimize the ground plane at the same time, we choose the length of the ground plane as 16 mm.

The return loss curves in Fig. 4 are calculated under the condition of all the other parameters are kept constant, and we only change the radii of the inner and outer rings. From this figure, we can see that the splitting ring loop structure has the characteristic of ultrawideband, and there are some apparent resonances in the working band. Cascading these three pairs of SRLs may be able to enhance the bandwidth and improve the frequency performance at the same time, and a new structure is proposed in Fig. 5.

In the design of a CPW-fed monopole antenna, the distance between the outer ring and the ground plane is a sensitive parameter that will affect the frequency performance. In order to obtain a very wide working band, the value of D_3 should be optimized. As can be seen from Fig. 6, the return losses of five different cases are similar when the frequency is less than 10 GHz. As the frequency increases, the return loss will be affected greatly with different values of D_3 , especially in the frequency band from 12 to 20 GHz. Simulations have shown that when the distance of D_3 is 0.22 mm, a relative better curve of return loss is obtained at the frequency band of 12 to 20 GHz.

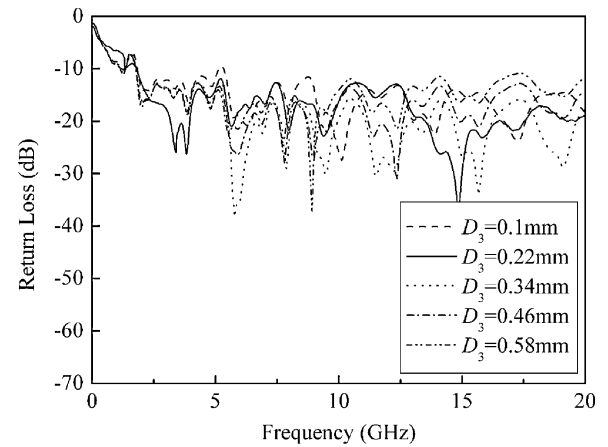


Fig. 6. Simulated return loss with different values of D_3 .

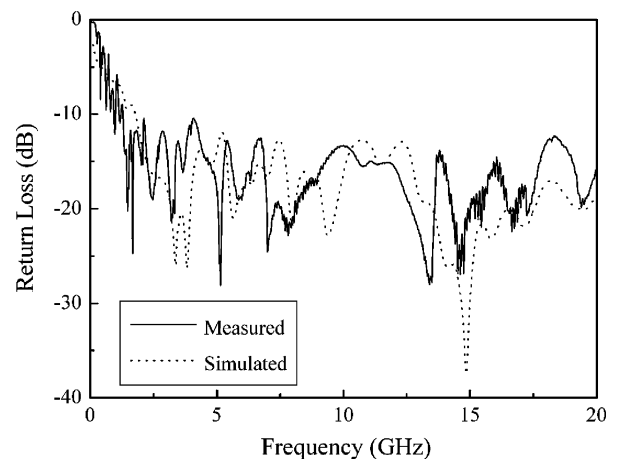


Fig. 7. Comparison between the measured and simulated results.

With the above analysis and optimization, we choose $D_3 = 0.22$ mm and the dimension of each split-ring loop varies proportionally to the arithmetic progression sequence. In this paper, a tapered transmission line is adopted to improve the return loss performance in the required band. The width of the tapered transmission line at the feed point is 3.15 mm, and it decreases 0.3 mm between every two neighbor rings (from the sixth ring to the central one).

III. NUMERICAL AND EXPERIMENTAL RESULTS

By optimization and comparison, we have a UWB antenna which consists with three pairs of split-ring loops, a tapered transmission line on the topside of the circuit board and two rectangular patches as the ground plane. The designed UWB antenna is fabricated on a substrate with the thickness of 1.0 mm and relative dielectric constant of 2.65. The frequency characteristic of the designed antenna is measured with Agilent 8722ES network analyzer (NA). Fig. 7 shows the measured results. In order to compare the experimental results with the analysis in Section II, the simulated results of the UWB antenna are also given in the same figure. From the measured results we can see that the fabricated UWB antenna has a measured band from 2.0 to 20 GHz. The return loss is better than -10 dB in the whole band.

The radiation patterns, transfer function and gain of the proposed UWB antenna were measured in anechoic chamber. The simulated and measured radiation patterns on the x-z plane and x-y plane for 3, 7, 10, and 15 GHz are shown in Fig. 8(a), (b), (c), and (d), respectively. It can be seen from the above figures that the measured results of x-y plane

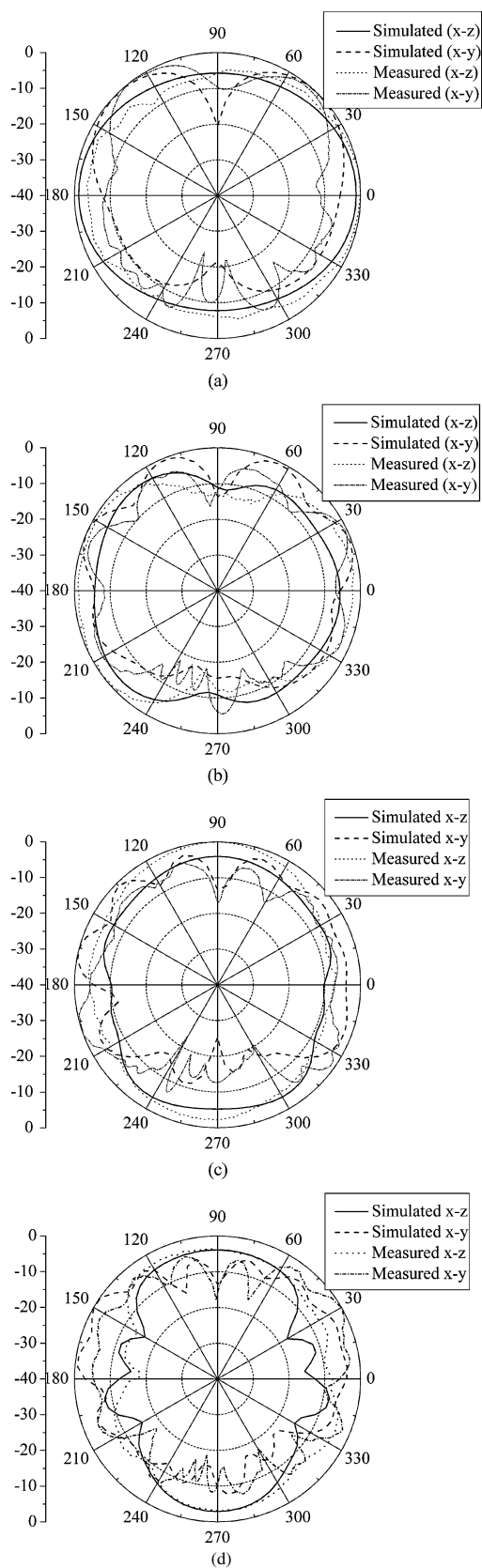


Fig. 8. The comparison between the measured and simulated radiation patterns. (a) 3 GHz. (b) 7 GHz. (c) 10 GHz. (d) 15 GHz.

show high directivity at low frequency and multidirectivities with the increase of frequency. Both the simulated and measured results of x-z

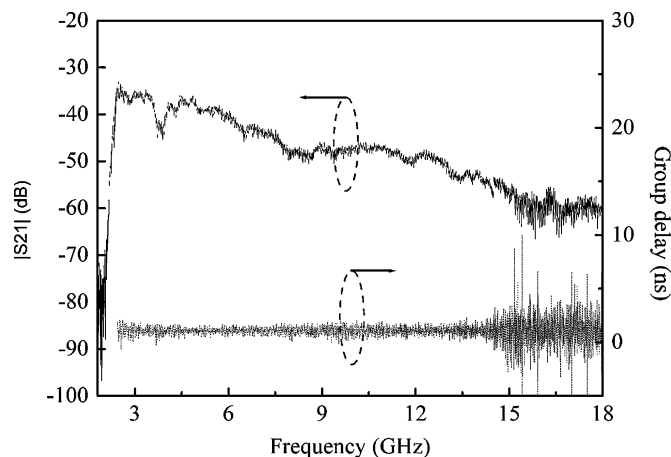


Fig. 9. Measured magnitude and group delay of the transfer function.

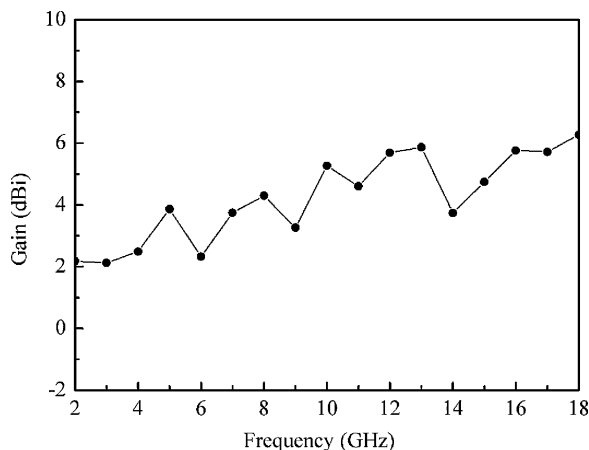


Fig. 10. Measured gain of the proposed UWB antenna.

plane show that proposed antenna exhibits nearly omnidirectional radiation pattern at low frequency. While at high frequency, the radiation patterns begin to change and show higher directivities in several directions because of the changes of the electrical dimensions of the antenna and ground planes.

The transfer function is presented in Fig. 9 for a distance of 1.5 m between the transmitter and receiver antennas located in an anechoic chamber. The measurement was carried out under the condition of two antennas facing each other in the direction of maximum radiation. As shown in Fig. 9, the graph of the magnitude versus frequency is relatively smooth in the working band ranging from 2 to 18 GHz, except that there are some dented points of $|S_{21}|$ between 3.5 to 4.5 GHz, which may be caused by the losses or a shift in the radiation pattern. Also from Fig. 9 we can see that the transfer function of the designed antennas has a flat group delay, which means that the UWB antennas have good transient response in the working band.

The measured antenna gain is shown in Fig. 10. From this figure we can see that in the whole UWB frequency, the whole tendency of the antenna gains raise with the frequency increases from 2 to 18 GHz. The average measured value of the gain is 3.99 dB, and the maximum and the minimum measured gains are 6.2 and 2.1 dB at 18 and 3 GHz, respectively.

IV. CONCLUSION

A new multiresonant split-ring loops UWB antenna has been successfully designed, fabricated and tested in this communication. The

designed antenna consists of three pairs of split-ring loops and a tapered transmission line. The simulated and measured results show that the proposed UWB antenna has a wide bandwidth from 2 to 20 GHz, and all the measured return losses are less than -10 dB in this band. The graph of the magnitude of the transfer function is relatively smooth combined with a flat group delay in the measured band. The simple planar geometry also makes it compatible with the existing microwave integrated circuit.

REFERENCES

- [1] K. L. Wong, *Compact and Broad-Band Microstrip Antennas*. New York: Wiley, 2002.
- [2] D. Kwon and Y. Kim, "Suppression of cable leakage current for edge-fed printed dipole UWB antennas using leakage-blocking slots," *IEEE Antennas Propag. Lett.*, vol. 5, pp. 183–186, 2006.
- [3] Z. N. Chen, "Novel bi-arm rolled monopole for UWB applications," *IEEE Trans. Antennas Propag.*, vol. 53, no. 2, pp. 672–677, Feb. 2005.
- [4] J. Liang, C. Chiau, X. Chen, and C. G. Parini, "Study of a printed circular disc monopole antenna for UWB systems," *IEEE Trans. Antennas Propag.*, vol. 53, no. 11, pp. 3500–3504, Nov. 2005.
- [5] J. Liang, L. Guo, C. C. Chiau, X. Chen, and C. G. Parini, "Study of CPW-fed circular disc monopole antenna," *IEE Proc. Microw., Antennas Propag.*, vol. 152, no. 6, pp. 520–526, Dec. 2005.
- [6] Q. Wu, R. H. Jin, J. P. Geng, and M. Ding, "CPW-fed quasi circular monopole with very wide bandwidth," *Electron. Lett.*, vol. 43, no. 2, pp. 69–70, Feb. 2007.
- [7] M. Ding, R. H. Jin, J. P. Geng, and Q. Wu, "Design of a CPW-fed ultrawide band fractal antenna," *Microw. Opt. Technol. Lett.*, vol. 49, no. 1, pp. 173–176, Jan. 2007.
- [8] N. Behdad and K. Sarabandi, "A multiresonant single-element wide-band slot antennas," *IEEE Antennas Propag. Lett.*, vol. 3, pp. 5–8, 2004.
- [9] K. Chang, *Microwave Ring Circuits and Antennas*. New York: Wiley, 1996.
- [10] J. S. Chen, "Dual-frequency annular-ring slot antennas fed by CPW feed and microstrip line feed," *IEEE Trans. Antennas Propag.*, vol. 53, no. 1, pp. 569–571, Jan. 2005.

Antenna Optimization With a Computationally Efficient Multiobjective Evolutionary Algorithm

Matthias John and Max J. Ammann

Abstract—An efficient multiobjective evolutionary algorithm is described for optimizing a novel spline based printed monopole antenna. The antenna geometry is based on spline outlines. Both radiating element and groundplane are simultaneously optimized by the algorithm. The resulting antenna performance is evaluated. It is shown that the evolutionary algorithm and the spline geometry can be used to efficiently generate ultrawideband antennas on limited computing resources.

Index Terms—Antenna optimization, multiobjective evolutionary algorithm, ultrawideband (UWB) antenna, spline.

I. INTRODUCTION

Evolutionary optimization methods such as genetic algorithms (GAs) and particle swarm optimization (PSO) have successfully been used to solve electromagnetic problems. These techniques have received great attention because they can solve a variety of problems and are easy to implement.

These algorithms start with solutions placed randomly in the search space and then evolve towards an optimum. Goodness of the solutions is assessed by a fitness function. This fitness function is usually computed from the results of a commercial or custom built electromagnetic solver.

The time these solvers need to compute the fitness of one trial solution varies from a few seconds to tens of minutes. The optimization algorithm has to trigger the solver hundreds or thousands of times during its run. For example, GAs have been reported [1]–[5] which run populations of 20–60 over 40–600 generations; thus needing up to 30000 function evaluations. Reported PSOs [6]–[8] evolve swarms of 10–800 for 1000–10000 iterations. The maximum number of times the EM solver is run in the cited papers is 200000. The total number of evaluations has to be weighted against the time per evaluation needed by the solver. Also, parallelization and the number of available computers have to be taken into consideration when choosing the setup for the algorithms.

This paper adopts an efficient global optimizer (EGO) reported by Joshua Knowles in [9]. This algorithm is designed to solve multiobjective optimization problems where each function evaluation is temporally or otherwise expensive. With the time taken by an EM solver being typically in the order of minutes, electromagnetic problems are ideal candidates for this optimization algorithm. The algorithm is suited for scenarios where computational power is limited or only a single license for commercial electromagnetic code is available, and thus, parallelization is not an option. The cited paper [9] compares the ParEGO to different GAs on a number of different theoretic problems, illustrating the performance benefits of ParEGO.

The algorithm selects the trial solution which is most likely to improve the best fitness before evaluation with the time expensive EM

Manuscript received November 21, 2007; revised July 03, 2008. Current version published March 04, 2009.

The authors are with the Centre for Telecommunications Value-chain Research, School of Electronic and Communications Engineering, Dublin Institute of Technology, Dublin 8, Ireland (e-mail: ammann@ieee.org).

Color versions of one or more of the figures in this comment are available online at <http://ieeexplore.ieee.org>.

Digital Object Identifier 10.1109/TAP.2008.2009775